A Benchtop Method for the Fabrication and Patterning of Nanoscale Structures on Polymers

3 AUTHORS, INCLUDING:

Charles Michael Drain

City University of New York - Hunter College

118 PUBLICATIONS **3,927** CITATIONS

SEE PROFILE

James D Batteas

Texas A&M University

91 PUBLICATIONS **2,748** CITATIONS

SEE PROFILE

A Benchtop Method for the Fabrication and Patterning of Nanoscale Structures on Polymers

James M. Helt,[†] Charles M. Drain,[‡] and James D. Batteas*,[†,§]

Contribution from the Department of Chemistry, College of Staten Island and the Graduate Center of the City University of New York, 2800 Victory Boulevard, Staten Island, New York 10314, and Department of Chemistry, Hunter College and the Graduate Center of the City University of New York, 695 Park Avenue, New York, New York 10021

Received March 13, 2003; E-mail: james.batteas@nist.gov

Abstract: A benchtop method for the facile production of nanoscale metal structures on polymers is demonstrated. This approach allows for the design and patterning of a wide range of metallic structures on inexpensive polymer surfaces, affording the fabrication of nanoscaled platforms for use in the design of sensors, actuators, and disposable electronic and photonic devices. Numerous structures, from simple nanowires to multilayered metallic gratings, are demonstrated, with sizes ranging from microns to the nanoscale. The process involves molding a malleable metal film deposited on a rigid substrate such as mica, by the compression of a plastic polymer stamp with the desired pattern against the metal film. While under compression, an etchant is then used to modify the metal. Upon separation of the stamp from the support, micro- to nanoscaled metallic structures are found on the stamp and/or on the substrate. The sizes of the structures formed depend on the sizes of the features on the stamp but can be fine-tuned by about 4-fold through variations in both pressure and duration of etching. Also, depending on the processing, multiple dimension metallic structures can be obtained simultaneously in a single stamping procedure. The metallic structures formed on the stamp can also be subsequently transferred to another surface allowing for the construction of multilayered materials such as band gap gratings or the application of electrical contacts. Using this approach, fabrication of both simple and complex micro- to nanoscaled structures can be accomplished by most any researcher as even the grating structure of commercial compact disks may be used as stamps, eliminating the requirement of expensive lithographic processes to form simple structures.

Introduction

The drive to economically reduce electronic and sensor architectures to the nanometer level has prompted a creative surge in soft lithographic techniques.[1,2] These include micro-contact printing (μCP),[3−9] nanoimprint lithography (NIL),[10−18] soft molding,[19] reverse NIL,[20] laser-assisted direct imprint (LADI),[21] cold welding nanotransfer,[22] lithography controlled wetting,[23] superlattice nanowire pattern transfer (SNAP),[24] nanotransfer printing (nTP),[25−27] molecular transfer lithography (MxL),[28] and micromolding in capillaries (MIMIC).[29−32] The processing requirements of each method (e.g., chemical

---

[†] College of Staten Island and the Graduate Center of the City University of New York.

[‡] Hunter College and the Graduate Center of the City University of New York.

[§] Present address: NIST, 100 Bureau Drive Mailstop 8372, Surface and Microanalysis Science Division, Gaithersburg, MD 20899.

(1) Xia, Y. N.; Rogers, J. A.; Paul, K. E.; Whitesides, G. M. *Chem. Rev.* **1999**, *99*, 1823−1848.
(2) Zhao, X. M.; Xia, Y. N.; Whitesides, G. M. *J. Mater. Chem.* **1997**, *7*, 1069−1074.
(3) Goetting, L. B.; Deng, T.; Whitesides, G. M. *Langmuir* **1999**, *15*, 1182−1191.
(4) Michel, B.; Bernard, A.; Bietsch, A.; Delamarche, E.; Geissler, M.; Juncker, D.; Kind, H.; Renault, J. P.; Rothuizen, H.; Schmid, H.; Schmidt-Winkel, P.; Stutz, R.; Wolf, H. *IBM J. Res. Dev.* **2001**, *45*, 697−719.
(5) Ng, W. K.; Wu, L.; Moran, P. M. *Appl. Phys. Lett.* **2002**, *81*, 3097−3099.
(6) (a) Zhong, Z. Y.; Gates, B.; Xia, Y. N.; Qin, D. *Langmuir* **2000**, *16*, 10369−10375. (b) Moran, C. E.; Radloff, C.; Halas, N. J. *Adv. Mater.* **2003**, *15*, 804−807.
(7) Kumar, A.; Whitesides, G. M. *Appl. Phys. Lett.* **1993**, *63*, 2002−2004.
(8) Schmid, H.; Michel, B. *Macromolecules* **2000**, *33*, 3042−3049.
(9) St. John, P. M.; Craighead, H. G. *Appl. Phys. Lett.* **1996**, *68*, 1022−1024.
(10) Chou, S. Y.; Krauss, P. R.; Renstrom, P. J. *Appl. Phys. Lett.* **1995**, *67*, 3114−3116.

(11) Chou, S. Y.; Krauss, P. R.; Renstrom, P. J. *J. Vac. Sci. Technol., B* **1996**, *14*, 4129−4133.
(12) Chou, S. Y.; Krauss, P. R.; Renstrom, P. J. *Science* **1996**, *272*, 85−87.
(13) Krauss, P. R.; Chou, S. Y. *Appl. Phys. Lett.* **1997**, *71*, 3174−3176.
(14) Wu, W.; Cui, B.; Sun, X. Y.; Zhang, W.; Zhuang, L.; Kong, L. S.; Chou, S. Y. *J. Vac. Sci. Technol., B* **1998**, *16*, 3825−3829.
(15) Li, M. T.; Chen, L.; Chou, S. Y. *Appl. Phys. Lett.* **2001**, *78*, 3322−3324.
(16) Austin, M. D.; Chou, S. Y. *Appl. Phys. Lett.* **2002**, *81*, 4431−4433.
(17) Cao, H.; Yu, Z. N.; Wang, J.; Tegenfeldt, J. O.; Austin, R. H.; Chen, E.; Wu, W.; Chou, S. Y. *Appl. Phys. Lett.* **2002**, *81*, 174−176.
(18) Austin, M.; Chou, S. Y. *J. Vac. Sci. Technol., B* **2002**, *20*, 665−667.
(19) Kim, Y. S.; Park, J.; Lee, H. H. *Appl. Phys. Lett.* **2002**, *81*, 1011−1013.
(20) Huang, X. D.; Bao, L. R.; Cheng, X.; Guo, L. J.; Pang, S. W.; Yee, A. F. *J. Vac. Sci. Technol., B* **2002**, *20*, 2872−2876.
(21) Chou, S. Y.; Keimel, C.; Gu, J. *Nature* **2002**, *417*, 835−837.
(22) Kim, C.; Shtein, M.; Forrest, S. R. *Appl. Phys. Lett.* **2002**, *80*, 4051−4053.
(23) Cavallini, M.; Biscarini, F. *Nano Lett.* **2003**, *3*, 1269−1271.
(24) Melosh, N. A.; Boukai, A.; Diana, F.; Gerardot, B.; Badolato, A.; Petroff, P. M.; Heath, J. R. *Science* **2003**, *300*, 112−115.
(25) Loo, Y. L.; Willett, R. L.; Baldwin, K. W.; Rogers, J. A. *J. Am. Chem. Soc.* **2002**, *124*, 7654−7655.
(26) Matsui, S.; Igaku, Y.; Ishigaki, H.; Fujita, J.; Ishida, M.; Ochiai, Y.; Namatsu, H.; Komuro, M. *J. Vac. Sci. Technol., B* **2003**, *21*, 688−692.
(27) Loo, Y. L.; Willett, R. L.; Baldwin, K. W.; Rogers, J. A. *Appl. Phys. Lett.* **2002**, *81*, 562−564.
(28) Schaper, C. D. *Nano Lett.* **2003**, *3*, 1305−1309.

treatments, temperatures, and pressures) as well as substrate compatibility are generally the limiting factors that narrow the range of materials that can be prepared by any single method mentioned above. For example, while most of these methods can be used to form metal nanostructures on planar[4,12,22,25,28,33] and/or curved surfaces,[34,35] the formation of patterned arrays of organic and inorganic molecules and particles are more readily obtained with capillary condensation,[23,36] MIMIC,[2,29–32,37–40] and μCP.[3,5–7,41–45] These methods may be combined by sequential implementation to provide several routes for the construction of multilevel, multiple composition nano-structured frameworks. An additional driving force for the continued development of soft lithographic techniques is that an economic advantage can be provided by methods which enable direct transfer of patterned materials to other substrates (via either additive or subtractive processes) without the need for additional chemical treatments. This reduces the number of processing steps, the associated production of waste, and the inefficient use of materials from each step. Cold welding nanotransfer is one such example where direct transfer is possible, and this approach has proven to be compatible with the fabrication of organic-based components with potential use in the fabrication of molecular electronic devices.[22,46] Nano-transfer printing with chemically[25,27] and physically[28] driven interfacial "bonding" has also proven to be an effective means of metal surface patterning and has recently been illustrated for the formation of electrical test structures using self-assembled monolayers on surfaces such as GaAs.[47]

In this paper, we present a method for the synthesis and transfer of materials to and from polymers (STOMP), which may find applications in constructing sensors,[48] electronic devices,[49] optical materials,[50,51] photolithography masks,[52] and layered photonic band gap structures.[53] As with many other soft lithographic (SL) techniques, STOMP utilizes preferential surface "modification" with a structured polymeric stamp in order to direct the formation of metal structures onto the stamp or substrate surface. The stamp geometry, interfacial free energies (hydrophilic/hydrophobic interactions) and applied loads cooperate to guide the resulting metal feature size. This benchtop route allows for the fabrication of multiple metal micro/nanostructures within the recesses and/or on the raised portions of a polymer stamp without the need for the addition of an "adhesive" layer to direct the transfer of materials to the polymer stamp. Although other techniques such as μCP are also capable of varying structural dimension (i.e., reducing feature size) by etching, the ability to directly produce and transfer metal arrays to a structured polymer in a single step is difficult to generate with other methods. The structures formed on the polymer stamps by the STOMP processes can also be subse-quently transferred to other surfaces allowing the fabrication of multilayered structures, such as metallic gratings with nanoscale dimensions.

Experimental Section

General Patterning Process. In the STOMP method, nanostructures are formed by the compression of a malleable metal film (such as Au) deposited on a rigid support (such as mica) by a polymer stamp followed by chemical etching while the metal film is under compression by the stamp. The STOMP processing begins by initially wetting the Au and polymer surfaces with ultrapure water (EASYpure RF, 18.2 MΩ cm, Barnstead, Dubuque, IA), methanol (Fisher Scientific), or a 1:1 v/v water/methanol mixture before compression to suppress bubble forma-tion between the stamp and substrate and to reduce the surface tension between the water-based etchant and hydrophobic stamp. The samples were etched while under compression with Transene gold etchant type TFA (Danvers, MA), which was diluted with ultrapure water in ratios ranging from 2:3 to 1:12.5 v/v TFA/H_2O. Custom-built Teflon compression cells designed to hold ~1 cm^2 samples were used to compress polymer stamps against the Au coated surfaces under a fixed uniform load. After securing the components, the compression cells were immersed in 100 mL of the gold etchant solution. Etching was carried out at room temperature (22 ± 3 °C) with rapid stirring from ~4–72 h, with a typical etching time of 20 h. Heating of the solution up to 70 ± 2 °C could also be used to reduce the required etching times. After etching, the compression cell was dismantled and the sample removed and rinsed with a solvent, such as methanol, to facilitate the separation of the two surfaces and to reduce disruption of the Au nanostructures formed. The polymeric stamp and substrate were then gently rinsed with copious amounts of ultrapure H_2O and dried under vacuum (~10 mTorr) at room temperature. The resulting structures were then characterized with scanning electron microscopy (SEM) and atomic force microscopy (AFM).

Fabrication of Polymer Stamps. Several different polymer stamps were used in this work. Micromolded polystyrene (PS) (MW of 235 000, Scientific Polymer Products Inc., Ontario, NY) stamps were fabricated by molding from a master silicon grating (such as TGG01, MikroMasch, Portland, OR), with an active area of ~9 mm^2 or from a silicon AFM calibration standard (Veeco/TM Microscopes, Sunnyvale, CA), with an active area of ~20 mm^2. The polymer stamps were formed by placing the silicon template face up in an aluminum or Teflon cell with ~0.5 g of PS placed over the template. The cell was then heated to 210 °C for 2 h and allowed to cool to room temperature. The PS

(29) Kim, E.; Xia, Y. N.; Whitesides, G. M. *J. Am. Chem. Soc.* **1996**, *118*, 5722–5731.
(30) Kim, E.; Xia, Y. N.; Whitesides, G. M. *Nature* **1995**, *376*, 581–584.
(31) Xia, Y. N.; Kim, E.; Whitesides, G. M. *Chem. Mater.* **1996**, *8*, 1558–1567.
(32) Pisignano, D.; Sariconi, E.; Mazzeo, M.; Gigli, G.; Cingolani, R. *Adv. Mater.* **2002**, *14*, 1565–1567.
(33) Odom, T. W.; Love, J. C.; Wolfe, D. B.; Paul, K. E.; Whitesides, G. M. *Langmuir* **2002**, *18*, 5314–5320.
(34) Paul, K. E.; Prentiss, M.; Whitesides, G. M. *Adv. Funct. Mater.* **2003**, *13*, 259–263.
(35) Rhee, K. W.; Shirey, L. M.; Isaacson, P. I.; Komegay, C. F.; Dressick, W. J.; Chen, M. S.; Brandow, S. L. *J. Vac. Sci. Technol., B* **2000**, *18*, 3569–3571.
(36) Moran, P. M.; Lange, F. F. *Appl. Phys. Lett.* **1999**, *74*, 1332–1334.
(37) Zhang, F. L.; Nyberg, T.; Inganas, O. *Nano Lett.* **2002**, *2*, 1373–1377.
(38) Kenis, P. J. A.; Ismagilov, R. F.; Takayama, S.; Whitesides, G. M.; Li, S. L.; White, H. S. *Acc. Chem. Res.* **2000**, *33*, 841–847.
(39) Pisignano, D.; Gigli, G.; Visconti, P.; Zocco, A.; Perrone, A.; Cingolani, R. *J. Vac. Sci. Technol., B* **2002**, *20*, 2248–2251.
(40) Wu, H. K.; Odom, T. W.; Chiu, D. T.; Whitesides, G. M. *J. Am. Chem. Soc.* **2003**, *125*, 554–559.
(41) Koide, Y.; Such, M. W.; Basu, R.; Evmenenko, G.; Cui, J.; Dutta, P.; Hersam, M. C.; Marks, T. J. *Langmuir* **2003**, *19*, 86–93.
(42) Zangmeister, R. A. P.; O'Brien, D. F.; Armstrong, N. R. *Adv. Funct. Mater.* **2002**, *12*, 179–186.
(43) Csucs, G.; Kunzler, T.; Feldman, K.; Robin, F.; Spencer, N. D. *Langmuir* **2003**, *19*, 6104–6109.
(44) Li, H. W.; Muir, B. V. O.; Fichet, G.; Huck, W. T. S. *Langmuir* **2003**, *19*, 1963–1965.
(45) Martin, B. D.; Brandow, S. L.; Dressick, W. J.; Schull, T. L. *Langmuir* **2000**, *16*, 9944–9946.
(46) Kim, C.; Forrest, S. R. *Adv. Mater.* **2003**, *15*, 541–545.
(47) Zaumseil, J.; Meitl, M. A.; Hsu, J. W. P.; Acharya, B. R.; Baldwin, K. W.; Loo, Y. L.; Rogers, J. A. *Nano Lett.* **2003**, *3*, 1223–1227.
(48) Li, C. Z.; He, H. X.; Bogozi, A.; Bunch, J. S.; Tao, N. J. *Appl. Phys. Lett.* **2000**, *76*, 1333–1335.
(49) Wind, S. J.; Appenzeller, J.; Martel, R.; Derycke, V.; Avouris, P. *J. Vac. Sci. Technol. B* **2002**, *20*, 2798–2801.
(50) Schider, G.; Krenn, J. R.; Gotschy, W.; Lamprecht, B.; Ditlbacher, H.; Leitner, A.; Aussenegg, F. R. *J. Appl. Phys.* **2001**, *90*, 3825–3830.
(51) Kreiter, M.; Mittler, S.; Knoll, W.; Sambles, J. R. *Phys. Rev. B* **2002**, *65*, art. no. 125415.
(52) Schmid, H.; Biebuyck, H.; Michel, B.; Martin, O. J. F. *Appl. Phys. Lett.* **1998**, *72*, 2379–2381.
(53) Aoki, K.; Miyazaki, H. T.; Hirayama, H.; Inoshita, K.; Baba, T.; Shinya, N.; Aoyagi, Y. *Appl. Phys. Lett.* **2002**, *81*, 3122–3124.

stamp was then separated from the silicon template with brief sonication (~2 min) in methanol and subsequently rinsed with ultrapure water. In addition to fabricated stamps, delaminated, commercially available recordable polycarbonate (PC) compact disks (CDs) could also be employed as stamps. CDs have been used as stamps in several patterning methods[54,55] and are also suitable stamps for STOMP. The CD stamps were prepared by removing the reflective metallic layer via scoring and vigorous rinsing with ultrapure water. The recording media was then removed with a rapid methanol rinse followed by brief sonication (~30 s) in a 1:4 (v/v) methanol/water solution and a final rinse with ultrapure water. The stamps were then cut to the desired size.

Formation of Au Films. Gold (Au) films were prepared with a sputter coater (BAL-TEC MED 020, Liechtenstein, Germany). The Au target (99.99% purity) was obtained from Techno Trade International (Manchester, NH). Substrates coated with Au included freshly cleaved muscovite mica (Structure Probe Inc., West Chester, PA), glass coverslips (Fisher Scientific), and Si(100) wafers (Virginia Semiconductor, Fredericksburg, VA). The prepared films ranged from 70 to 300 nm in thickness with a deposition rate between 0.2 and 2 nm/s. The evaporated films exhibited a surface roughness of ~2−5 nm RMS.

Evaluation of Load Dependence on Pattern Formation. The compressive load dependence on the structures that could be formed using STOMP was evaluated using two approaches. First, using a simple sequential variation of the load in a series of experiments with a planar compression cell, whereby the pressure is nominally uniform across the stamp/substrate interface. The second uses a nonplanar compression configuration in which convex lenses acted as the compression plates (vide infra). This second approach has the advantage that using the curved compression geometry results in a radial pressure gradient at the stamp−substrate interface, which allows for an entire series of structure vs load to be evaluated in a single experiment. The normal load and pressure distribution could then be estimated with continuum contact mechanics theory (neglecting effects of the Au film[56−59]) as well by comparison to the observed deformation of the Au films and polymer stamps evaluated ex situ using a calibrated press.[60] The ex situ load dependent experiments evaluating deformation of the Au film by the polymer stamp were performed using a press employing a set of calibrated springs with a maximum load capacity of 153 ± 2 N.

Imaging. AFM images were acquired with either a Molecular Imaging Pico SPM (Phoenix, AZ) coupled with an RHK Technology SPM 1000 Controller, Revision 8 (Troy, MI), or a Park Scientific Autoprobe LS AFM (Veeco/TM Microscopes, Sunnyvale, CA). All AFM images were acquired in contact mode using commercially available Si_3N_4 AFM tips (Veeco/TM Microscopes, Sunnyvale, CA) with nominal tip radii of 10−30 nm and nominal spring constants of ~0.1 N/m. SEM images were obtained with an Amray 1800 (KLA Tencor, San Jose, CA). To minimize charging, the typical SEM imaging conditions used an electron beam current at the sample of ~110 μA with an acceleration voltage of 3.1 kV.

Results and Discussion

General Patterning Process. In the STOMP method (Figure 1), nanostructures are formed by compressing a polymer stamp against a thin metal film (such as Au) deposited on a rigid support (such as mica, glass or Si) followed by chemically etching the film while under compression. After rinsing, the polymer stamp and support are separated, yielding structures of the initial film material wherein the resulting organization is
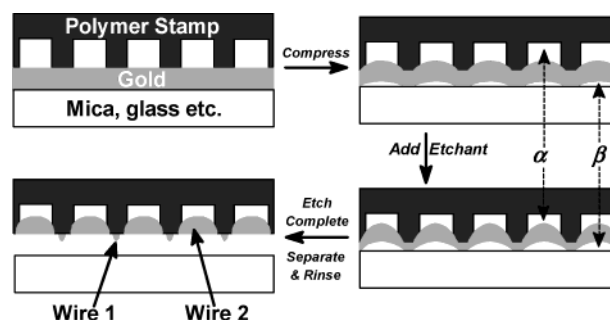

Figure 1. Schematic of the STOMP protocol using planar stamps with square sidewalls. A polymer stamp from a compact disk or prefabricated from a master template is brought into compressive contact with an Au film (typically 70−300 nm thick) on a rigid support such as mica, glass, or Si. Compression induces buckling in the Au film producing two channels, α and β. As the β channel is more hydrophilic than the α channel, etching occurs preferentially through the β channel and under the stamp ridges. After an etching step, the stamp and support are separated and rinsed. Depending on the duration of etching, Au micro/nanostructures form on the stamp ridges (wires 1) and/or within the stamp recesses (wires 2).

dictated by the combination of the initial relief structure of the stamp, the interfacial chemistry (i.e., surface energies), and the overall compressibility of the stamp/film/substrate contacts. Using the STOMP process, structures ranging from microscale to the nanoscale are formed and are typically found either on the supporting substrate or within the space defined by the stamp recesses, and/or on the protruding features of the polymer stamp. Subsequent transfer of nanostructures from one surface to another can be readily achieved and enables the construction of more complicated architectures such as 3D superlattices. There are several architectures that can be fabricated by STOMP, and these can be described in three main classes: (1) embedded metal structures, (2) binary structures, and (3) multilayered structures. The structures formed are dependent upon the initial morphology of the stamp used, the pressure with which the stamp and substrate are compressed, and the length of time the samples are etched. In the work presented here, we employed two general types of stamps, those with saw-tooth structures and those with flat planar, ridged structures, consisting of raised lines, cylinders, or crosshatched lines. Examples of the types of structures that can be fabricated using these stamps are described, as well as the impact of processing on the resulting structures.

Patterning with Planar Stamps. When polymer stamps with flat rectangular profiles such as those found on a compact disk (CD) are compressed against a ~70 nm thick Au film on rigid supports such as mica (Figure 2), the Au structures produced are embedded in the stamp recesses after complete etching. Compression of the stamp against the Au film induces buckling, forcing the Au film to deform and to be thinned and displaced from under the ridges of the stamp up into the recesses (Figure 2b), delaminating from the substrate under these regions. This deformation and delamination of the film yields two channels (α and β). Such lifting of a "nonbonded" metal film under loading can occur when the layer thickness is less than the contact width.[61−63]

The two channels (α and β) formed during compression can be exploited to introduce a preferential etch in one channel (β)

(54) Yu, H. Z. *Anal. Chem.* **2001**, *73*, 4743−4747.
(55) Yu, H. Z.; Rowe, A. W.; Waugh, D. M. *Anal. Chem* **2002**, *74*, 5742−5747.
(56) Meijers, P. *Appl. Sci. Res.* **1968**, *18*, 353−383.
(57) Alblas, J. B.; Kuipers, M. *Acta Mechanica* **1970**, *9*, 292−311.
(58) Alblas, J. B.; Kuipers, M. *Acta Mechanica* **1970**, *9*, 1−12.
(59) Alblas, J. B.; Kuipers, M. *Acta Mechanica* **1970**, *8*, 133−145.
(60) Johnson, K. L. *Contact Mechanics*; Cambridge University Press: Cambridge, 1987.

(61) Gladwell, G. M. L. *J. Appl. Mech.* **1976**, *43*, 263−267.
(62) Goudeau, P.; Villain, P.; Tamura, N.; Padmore, H. A. *Appl. Phys. Lett.* **2003**, *83*, 51−53.
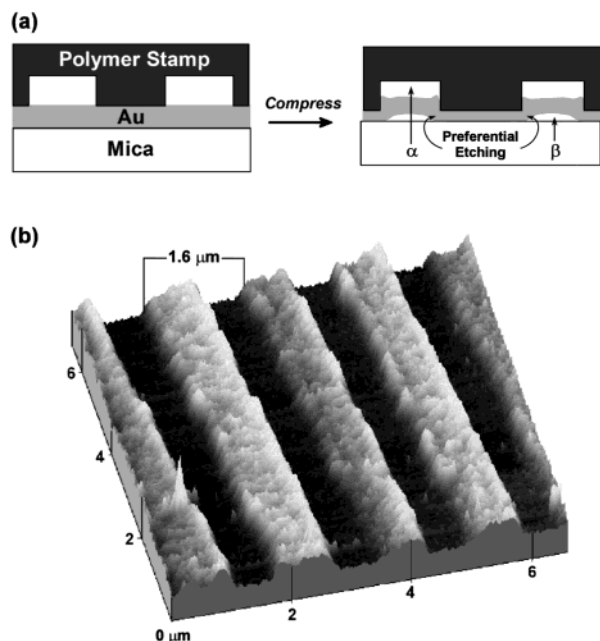(63) Keer, L. M.; Dundurs, J.; Tsai, K. C. *J Appl. Mech.* **1972**, *39*, 1115.

Figure 2. (a) Schematic of the plastic deformation that occues when the Au film is compressed by the stamp. Thinning of the Au film occurs under the ridges, causing it to buckle and delaminate under the recesses from the support ultimately forcing the Au into the recesses of the stamp. (b) An AFM image of a 70 nm Au film on a PC stamp after compression using a typical load of 144 $\pm$ 2 N (corresponding to a mean pressure of ca. 69 MPa acting at the stamp–substrate sandwich interface) applied for 12 h without etching. This shows that the initial 70 nm thick Au film has been thinned and raised into the stamp recesses after STOMP processing.

Table 1. Surface Energies of the Polymers and Substrates Employed in This Work

material	γ (mN/m)
gold	1145 (50 °C)[73]
mica	144 (22 °C)[74]
polystyrene (PS)	40.7 (20 °C)[71]
polycarbonate (PC)	42.9 (20 °C)[71]
octadecyltriethoxy silane (OTE)	22[75], 31[76] (25 °C)

over the other (α), based on the solid–liquid interfacial energies of the materials forming the two channels (Table 1).[64,65] Under typical processing conditions, the α channel is hydrophobic, as it is defined by the polymer–Au interface, while the β channel offers a more hydrophilic conduit due to the substrate (e.g., mica, glass or an oxidized silicon wafer). Consequently, during etching, the diffusion of the aqueous phase enchant through the α channel is restricted relative to the β channel. This provides a mass transport advantage within the β channel for selective chemical etching below the raised Au, most likely initiating at the pinched strained interface of the Au/mica junction. The phenomenology of arrested or enhanced fluid flow through micro channels[39,66,67] has been extensively investigated and exploited in micrototal analysis systems[68] and MIMIC replication techniques.[2,32,37–40] We have tested this argument of restricted flow and anisotropic etching in our patterning process by conducting experiments in which Au films were deposited

(64) deGennes, P. G. *Rev. Mod. Phys.* **1985**, *57*, 827–863.
(65) Myers, D. *Surfaces, Interfaces, and Colloids*; Wiley VCH: New York, 1999.
(66) Kim, D. S.; Lee, K. C.; Kwon, T. H.; Lee, S. S. *J. Micromech. Microeng.* **2002**, *12*, 236–246.
(67) Zhao, B.; Moore, J. S.; Beebe, D. J. *Anal. Chem.* **2002**, *74*, 4259–4268.
(68) Reyes, D. R.; Iossifidis, D.; Auroux, P. A.; Manz, A. *Anal. Chem.* **2002**, *74*, 2623–2636.
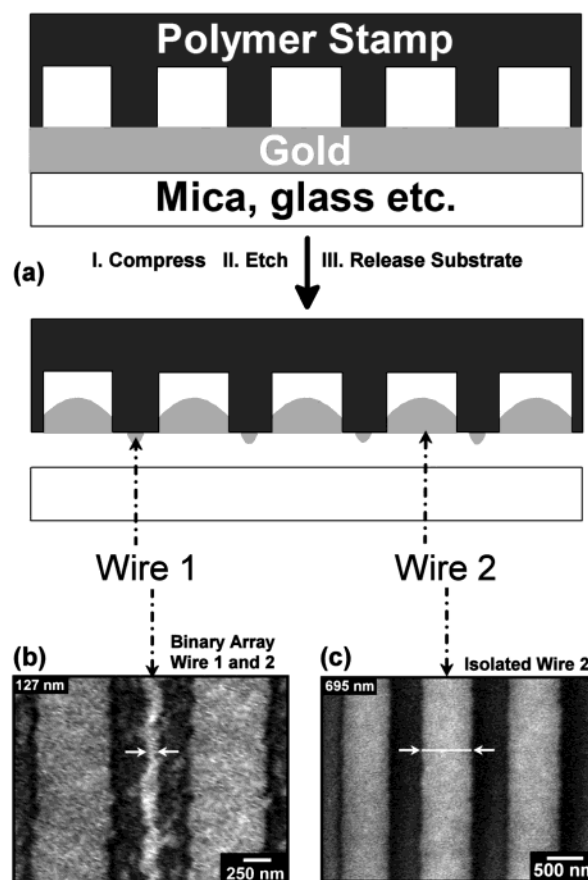
Figure 3. (a) Schematic illustrating the placement of the primary structures formed with a polymer stamp possessing a rectangular profile. Wire 1 resides on the raised stamp feature, while wire 2 is inlaid between the raised polymer stamp features. (b) SEM image of a binary gold wire array. Wires reside on the raised ($\sim$127 nm, wire 1) and within the recessed ($\sim$750 nm, wire 2) regions of a rectangular polycarbonate stamp. The binary wire array is found at the center of the stamp–Au film contact where etching has not completely removed the Au film from under the stamp ridges. (c) SEM image of isolated Au wires ($\sim$695 nm) embedded in the recesses of a polycarbonate stamp (wire 2) following complete etching. The embedded wires (wire 2) are continuous over the patterned area of $\sim$1 mm^2 and possess a maximum width variation of $\sim$11% across the surface.

on octadecyltriethoxysilane (OTE) coated silicon or glass substrates. With these surface modifications, both the α and β channels are rendered hydrophobic. Processing under these conditions, etching was found to be severely impeded, with only the outermost contact periphery between the stamp and Au surface showing any well-formed structures.

Thus under typical STOMP conditions with a hydrophilic substrate, the Au underneath the ridges of the polymer stamp are etched away faster as the continual compression induces thinning and strain of the delaminating film leaving most of the Au only within the recessed regions of the stamp. Once all of the Au under the stamp ridges has been etched away, embedded Au wires remain within the stamp recesses (Figure 3c, wire 2). Here we show Au wires embedded in the grating structure of a polycarbonate compact disk. The grating structure of the CD used here had $\sim$200 nm deep by $\sim$500 nm wide recesses and $\sim$1000 nm wide ridges. These recessed Au structures formed using this STOMP method are found by AFM to be nearly coplanar ($\pm$10 nm) with the polymer stamp ridges. The width of the final embedded gold wires are $\sim$695 nm. The lateral dimension of wire 2 is larger than the recess width
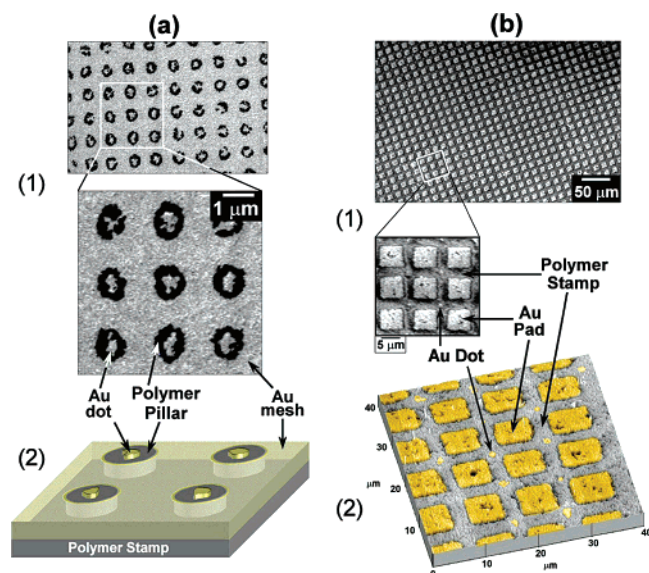
Figure 4. Patterns formed using polymer stamps with (a) cylindrical pillars and (b) square crosshatches. (a1) SEM images of a gold structure array consisting of 100 nm thick Au film encompassing pillars of a PS stamp. The dark, ~1 μm (2 μm pitch) circular features correspond to the upright polymer pillars within the Au film. (a2) When etching is stopped prior to completion of part a, Au "dots" are formed and rest on top of the polystyrene pillars. The nonuniform Au dot structure is attributed to the defects in the defining stamp topology yielding nonsymmetric etching. (b1) SEM images of 6 μm square (9 μm pitch) Au pads (100 nm thick Au) embedded within a polystyrene stamp matrix. An AFM image of the embedded Au pads shows a nearly coplanar arrangement (~9 nm RMS roughness) with the polystyrene matrix (b2). Au dots are found where the polymer edges intersect, when etching is incomplete (close-up, b1).

because the edges of the PC stamp ridges are actually deformed inward by the forced compression of the Au into the recesses. This makes the outer edges of the recesses wider, resulting in a slight overhang of Au over the ridges following etching. The dimensions of the wires across the entire area of the printed structure are found to be uniform to within ±11% of this size. Almost no variation of final feature size as a function of compressive load is observed, as the stamp ridges are flat and broad.

Using the same type of stamp but changing the duration of etching allows for the formation of binary structures, which consist of Au wires embedded *within* the recesses as well as resting *on top* of the stamp ridges. This occurs if the etching process is halted prior to the complete etching of Au from underneath the stamp ridges. Here we illustrate (Figure 3b) the simultaneous production of binary nanowire arrays, wherein ~127 nm wires are found on the raised features of the stamp (wire 1) and ~750 nm wires (wire 2) are found in the recessed features of the rectangular polymer stamp.

The same general principles of structure formation (i.e., Au is compressed into the recesses of the stamp, and etching occurs preferentially under the stamp ridges first) apply for other stamp geometries that also possess flat ridges with square sidewalls. For example, when a stamp with cylindrical posts is employed, complete etching forms a Au film with interstitial polymer pillars. Incomplete etching results in the formation of nanodots centered on top of the polymer pillars, and the rest of the Au film is in the recessed portions of the polymer stamp (Figure 4a). The observed formation of these types of structures further supports the mechanism mentioned above, that Au etching is initiated at the strained portions of the film while under compression, prompting accelerated etching along the periphery
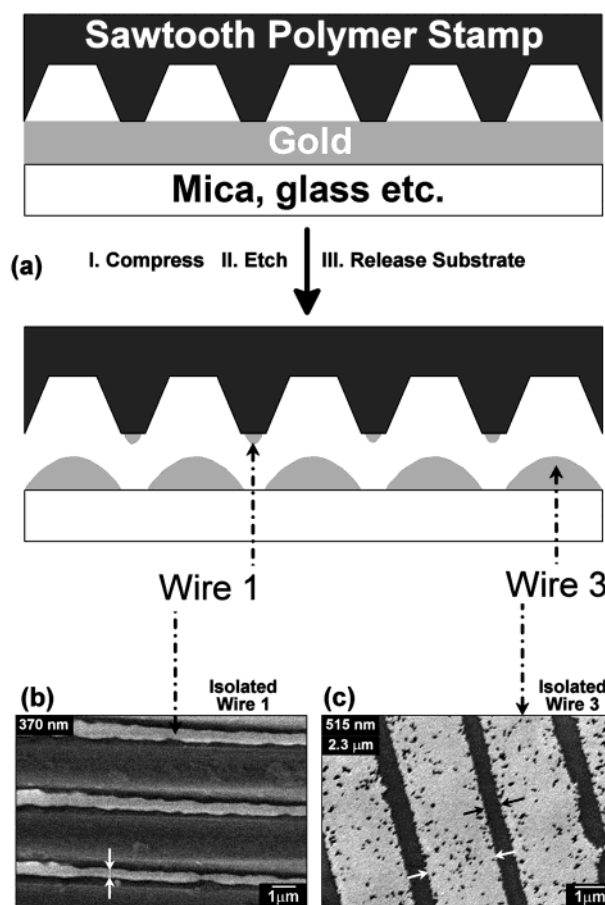

Figure 5. (a) Schematic illustrating the STOMP process using a polymer stamp possessing a saw-tooth profile. Upon separation of the stamp from the surface, two types of structures are formed (wires 1 and 3). Wire 1 resides on the raised stamp feature, while wire 3 remains on the substrate. (b) SEM image of Au wires (wire 1; ~370−600 nm) resting on the ridges of a saw-tooth polystyrene stamp with a 3 μm pitch after STOMP processing and (c) wire 3 complements remaining on the mica substrate. Etch pits are typically present in wire 3 as etching occurs through the channels formed by the Au/stamp interface.

of the stamp ridge contact where the tensile stresses are at a maximum.[60] When a crosshatched stamp with well separated square recesses is used, embedded square Au pads are formed with complete etching. When incomplete etching is carried out, Au dots are observed in the center of the intersections of the stamp ridges as well as the square pads in the recesses (Figure 4b).

Patterning with Saw-Tooth Stamp Structures. Switching to stamps with a saw-tooth structure offers an additional means of controlling the structures that can be fabricated. The saw-tooth stamp ridges are parabolic in shape with sloped sidewalls. To investigate the patterning of Au structures using a saw-tooth stamp, we fabricated a polystyrene stamp with ~1.3 micron high ridges (~3 micrometer pitch) with a radius of curvature of ~500 nm. When the curved edges of the stamp are compressed against the Au film under the same load conditions used for patterning with flat ridged stamps, the increased load per unit contact area for the saw-tooth stamps makes the contact pressure greater than the yield stress of the polymer, which partially flattens out the polymer ridges and protects the Au under the raised stamp features from etching. The protected portion of the Au film is subsequently transferred to the ridges of the contacting polymer stamp. The residual Au lying between
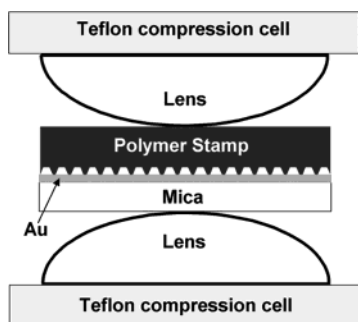
Figure 6. Schematic of the nonlinear compression configuration used, which employs two plano-convex lenses as the compression plates. This arrangement provides a well-defined point of contact with a load that varies radially, decreasing outward from the center of contact, permitting a means of investigating load dependence on the dimensions of STOMP fabricated gold structures in a single experiment.

stamp ridges remains on the substrate surface forming a patterned Au film on the support (Figure 5). Thus, with this type of stamp geometry, two distinct patterned products on opposing substrates may be formed simultaneously. The sloped sidewalls act to limit mechanical binding of the metal film effectively eliminating embedded product formation. Moreover, the volume of the channels formed at the Au/polymer interface with the saw-tooth stamps used here are at least 10 times greater than those in the planar cases described, whose channels were relatively small and partially filled with Au when compressed against the metal film. Thus, in this case, etching can more readily occur within the channels formed by the polymer/Au interface, as these channels are sufficiently large to afford transport of the etchant.

Using this stamp geometry, unlike stamps with planar features, the structures formed are dependent on the load applied in STOMP processing. The compressive load could be readily used to tune the dimensions of the structures transferred to the polymer stamp. If the parabolic stamp ridge/Au film contacts were perfectly elastic, one would expect the contact radius to be proportional to the applied load to the one-half power (based on the contact mechanics model of a cylinder against a flat plane) and the resulting feature widths produced would then follow a similar load dependence.[60] However, even though the channels in this stamp are fairly large, a geometric etch rate anisotropy induced by a free volume constraint on the etchant diffusion is often observed, whereby the etching was more complete at the edges of the stamp/Au contact than in the center of the stamp/Au contact. This results in a spatial variation by as much as 25% in the dimensions of the structures formed by this STOMP procedure due to etching alone. Thus under uniform compression, there is an inherent convolution of the applied load and the etching time which determines the size of the resulting structures. In light of this coupling between the etch rate and compressive load on the product feature size, we investigated the influence of pressure on the wire width by compressing the polymer stamp against the Au film between curved press plates made from plano-convex lenses (Figure 6). This compression geometry results in a radial pressure gradient at the stamp/Au contact allowing us to probe the load dependence on the structures formed using a single set of experimental conditions.[57,69] Here we again employed a saw-tooth stamp made of polystyrene with the same dimensions as described above. The resulting pressure distribution[70] is found to modulate the dimensions of the nanowires produced such that, under the highest pressures ($\sim$245 MPa), found in the center of the stamp/Au interface contact, wider wires are formed ($\sim$900 nm wide), while much thinner wires are found ($\sim$180 nm wide) at the edges of the contact where the pressures are less ($\sim$43 MPa) (Figure 7).
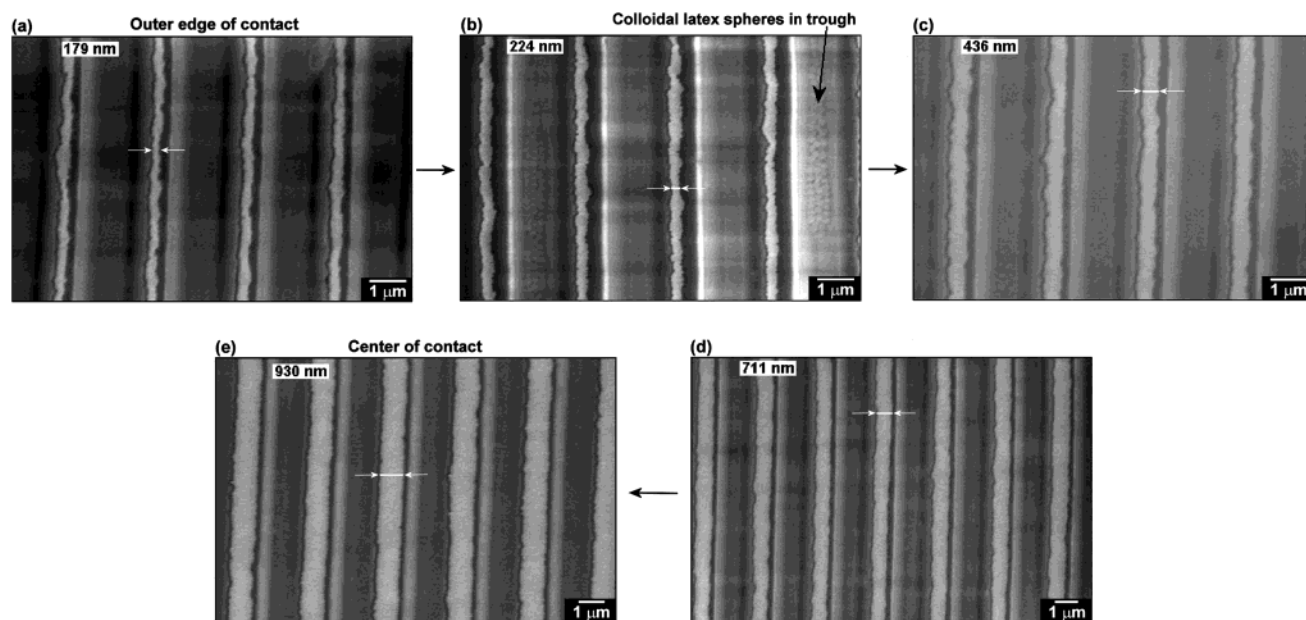

Figure 7. SEM images of a polystyrene stamp with gold wires on the ridges made by STOMP processing using opposing convex lenses (as in Figure 6). White arrows highlight the Au feature widths, and their dimensions are given in the upper left-hand corner of each image. Gold wires are arranged along the ridge of the polystyrene saw-tooth grating. The 200 nm colloidal latex particles in part b were solution deposited into the grating troughs to demonstrate the location of the Au wires. When using the opposing convex lenses to exert pressure on the stamp-gold−substrate sandwich, the saw-tooth stamp yields a wire width that varies radially, with (a) the thinnest wires ($\sim$180 nm) located at the edge of the stamp/film contact where the pressure is lowest and (e) the widest wires ($\sim$900 nm), located at the center of the contact where the pressure is highest. The separation from the center of contact to the outer edge shown here was $\sim$0.5 mm.
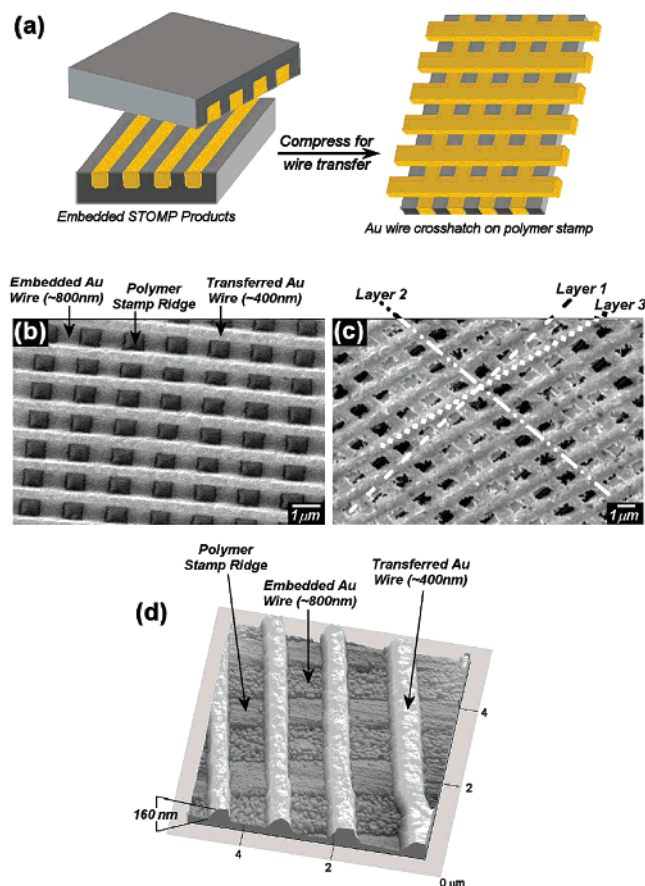
Figure 8. (a) Schematic illustrating cold-welding transfer of embedded Au wires. SEM images of (b) an Au wire bilayer with bottom and top wire widths equal to ∼800 and ∼400 nm, respectively, and (c) a trilayer crosshatch of Au wires are shown. Both multilayered architectures are created by bringing two polycarbonate stamps, possessing inlaid nanowire arrays (as in Figure 3c), into compressive contact. Cold welding enables transfer of the embedded wires from one stamp surface to another. (d) AFM image of the bilayer crosshatch (a) showing the nearly coplanar arrangement of embedded Au wire (∼800 nm wide) with the raised stamp features (∼400 nm wide).

Following patterning, 200 nm PS beads (which have greater affinity for the stamp surface than the Au surface) were added to the fabricated structure and are found to reside within the recesses of the stamp, further illustrating that the Au wires

transferred to the stamp appear on the ridges. In the example illustrated here, AFM images of the stamp ridges prior to compression possessed a radius of curvature of ∼500 nm. Thus, STOMP provides the ability to both magnify and reduce final structure size via control of the compression load, and it is easy to envision the capability for forming very narrow wires simply by using a molded stamp with sharper ridge features.

Formation of Multilayered Structures. Multilayered 3-D architectures, such as crosshatches, can also be achieved with STOMP by compressing two stamps with embedded wire products together (Figure 8). Transfer is predominantly observed to occur from the surface with the thinner wires to the surface with the thicker wires. This transfer process is driven by the higher cohesive energy of the Au−Au contacts (via cold welding) to that of the adhesion of the Au to the polymer stamp, as observed in nanotransfer printing.[22,25,27,28] No reagent, other than water for rinsing, is necessary to create these multilayered structures. The raised Au wires (wire 1) can also be transferred to another substrate such as poly(dimethylsiloxane) where adhesion to the secondary surface exceeds that of the original stamp. In this fashion, structures can be fabricated and then placed onto another surface affording additional design modality.

Summary

A method for the synthesis and transfer of materials to and from polymers (STOMP) has been developed. Features fabricated by STOMP are found to be strongly dependent on the structure of the polymer stamp and its mechanical properties, the compression of the metal film, and the respective interfacial forces between the stamp, film, and substrate. The structures produced are robust, with sufficient mechanical integrity to enable repeated transfer steps to easily build multilayered architectures. Complex nanostructures such as binary nanowire arrays, as well as wires with varying dimensions depending on pressure, have also been demonstrated. The ability of a single procedure to yield such a wide range of structures by simply changing stamp shape, compression geometry, and/or etching time makes the STOMP process attractive for the benchtop fabrication of many potential devices. This ability to fabricate structures using even simple compact disks as stamps make this a method that can be employed by any researcher without the need for complex fabrication facilities.

(69) Hertz, H. *J. Reine Angew. Math.* **1881**, *92*, 156−171.
(70) For simplicity, the Hertz model was used to estimate the relative pressure distribution produced by the lens at the stamp/metal contact (ref 69). The radius of curvature of the lens was ∼37 mm, and the measured contact diameter under compression was 1.32 mm. The respective Poisson ratio (ν) and Young's modulus (E) of the polystyrene stamp and silica lens were ($\nu_{PS} = 0.33$, $E_{PS} = 3.3$ GPa)(ref 71) and ($\nu_{silica} = 0.17$, $E_{silica} = 73$ GPa) (ref 72). Here we did not take into account the Au film or plastic effects such as strain hardening. The ridge contact width was assumed to vary radially in line with the macroscopic load distribution as well as with empirical wire width measurements. Although the actual pressures at the ridges are likely to deviate from the calculated values due to asperity flattening and plastic processes within the stamp and Au film, the values do illustrate the relative load differences between the center and edge of the contact, which produced the nearly 4-fold difference in wire dimension.
(71) Brandrup, J., Immergut, E. H., Eds.; *Polymer Handbook*, 3rd ed.; Wiley-Interscience: New York, 1989.
(72) Batteas, J. D.; Quan, X. H.; Weldon, M. K. *Tribol. Lett.* **1999**, *7*, 121−128.

(73) Vermaak, J. S.; Kuhlmann-Wilsdorf, D. *J. Phys. Chem-Us* **1968**, *72*, 4150−4154.
(74) Christenson, H. K. *J. Phys. Chem-Us* **1993**, *97*, 12034−12041.
(75) Kim, S.; Christenson, H. K.; Curry, J. E. *J. Phys. Chem. B* **2003**, *107*, 3774−3781.
(76) Ruths, M.; Granick, S. *Langmuir* **1998**, *14*, 1804−1814.